Modeling of Nanoindentation in Ni-Graphene Nanocomposites: A Molecular Dynamics Sensitivity Study

Vardan Hoviki Vardanyan
Physics Department and Research Center OPTIMAS, Technische Universität Kaiserslautern, Germany

Herbert M. Urbassek
Physics Department and Research Center OPTIMAS, Technische Universität Kaiserslautern, Germany

Abstract

Using molecular dynamics simulation, we perform nanoindentation simulations on a Ni-graphene model system, in which a graphene flake coats the grain boundary of a Ni bi-crystal. Material strengthening or weakening by inclusion of graphene is discussed with the help of the force needed to indent to a specified depth. By varying the depth of the graphene flake with respect to the indentation depth we identify the distance up to which graphene influences the indentation behavior. In addition, we vary the details of the modeling of the graphene flake in the matrix metal and determine their influence on the performance of the nanocomposite. Our results indicate that the modeling results are robust against variations in the modeling of the graphene flake.

2012 ACM Subject Classification Applied computing → Physical sciences and engineering

Keywords and phrases molecular dynamics, nickel-graphene composites, dislocations, nanoindentation

Digital Object Identifier 10.4230/OASIcs.iPMVM.2020.12

Funding We acknowledge the financial support of the Deutsche Forschungsgemeinschaft (DFG, German Research Foundation) – project number 252408385 – IRTG 2057.

Acknowledgements Simulations were performed at the High Performance Cluster Elwetritsch (RHRK, TU Kaiserslautern, Germany).

1 Introduction

Nanoindentation is a well-established tool for studying the strength of materials [4, 1]. Molecular dynamics simulation has been frequently employed to investigate the processes occurring under nanoindentation with atomistic detail [21, 20]. In ductile materials, it allows in particular to monitor the generation of dislocations during the indentation and their subsequent propagation into the material as well as dislocation reactions, annihilations or interactions with interfaces.

Recently, nanocomposite materials – and here in particular graphene-metal nanocomposites – came into the focus of research [5]. This class of materials uses graphene with its high in-plane elastic modulus and yield strength as a strengthening filler component in a metal matrix [19, 32, 28, 30]. For the understanding of plastic processes in this composite material, the interaction of dislocations with graphene flakes is relevant. Indeed, a number of simulation studies investigated this interaction. They found that as a rule graphene blocks the penetration of dislocations, thus increasing the density of dislocations near the indenter [14, 12, 3, 22]. However, the graphene interface may also absorb dislocations which eventually results in a wrinkling of the graphene layer [25].

2nd International Conference of the DFG International Research Training Group 2057 – Physical Modeling for Virtual Manufacturing (iPMVM 2020).
Editors: Christoph Garth, Jan C. Aurich, Barbara Linke, Ralf Müller, Bahram Ravani, Gunther Weber, and Benjamin Kirsch; Article No. 12; pp. 12:1–12:13

OpenAccess Series in Informatics
Schloss Dagstuhl – Leibniz-Zentrum für Informatik, Dagstuhl Publishing, Germany

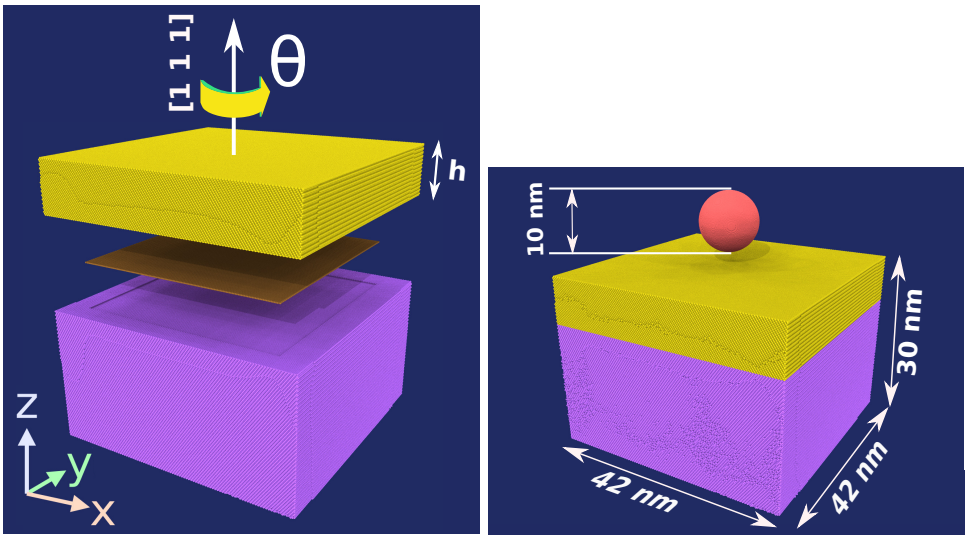

Figure 1 Left: Schematic setup of the bi-crystal used. The lower (purple) and the upper (yellow) Ni block are separated by a twist grain boundary with twist angle θ. In the grain boundary, a graphene layer (brown) is inserted. The Ni blocks have (111) surfaces. Right: Position of the indenter (red) at the beginning of the simulation and sizes of the simulation system.

In this paper, we will focus on Ni as matrix metal. Ni is a prominent matrix material and has been used in a variety of both experimental and computational studies of Ni-graphene nanocomposites [2, 11, 10, 15, 31, 16, 27, 25]. (111) surfaces of fcc metals have the same symmetry as graphene, and indeed often this is the preferred orientation of the metal-graphene interface [11]. However, because of the lattice mismatch between Ni and graphene, the interface is incoherent.

Recently, the hardness of Ni(100)-graphene [25] and Ni(111)-graphene [26] composites was studied in detail. As a model case, one may consider a Ni bi-crystal whose grain boundary is coated by a graphene flake. For this case, it could be concluded that the ideal Ni crystal is the hardest. Grain boundaries weaken it, in particular those with an incoherent and weak (i.e., high grain-boundary-energy) interface. The inclusion of graphene does not harden the composite, since (i) graphene is loaded perpendicular to its strong direction; (ii) it is opaque to dislocation slip, and dislocation absorption at the interface weakens the material; (iii) as soon as dislocations nucleate also in the lower Ni block, the indentation force is reduced. When the tip touches the graphene, it may result in interface failure, reducing the composite hardness. So in total, graphene addition does not strengthen the material in this model scenario.

In the present paper, we study to what extent details of the atomistic modeling affect the performance of the Ni-graphene interface in nanoindentation. To this purpose, we vary the exact positioning of the interface – both the depth of the graphene flake, its lateral position, and the orientation of the flake with respect of the Ni matrix – and study its influence on the nanoindentation. In addition, we also study how the interaction between graphene and Ni influences the results.

2 Simulation method

We use a Ni bi-crystal as simulation system, see Fig. 1. It has a (111) surface and contains a twist grain boundary. Two twist angles are studied in this work, $\theta = 60°$ and 30°. From a study of the grain boundary energy [17], is known that the 60° grain boundary is strong, while the 30° grain boundary is weak. The upper block has a height h which is taken to be 3, 5, and 8 nm. The entire Ni system has a a height of 30 nm and lateral extensions of 42 nm, containing approximately 4.9 million atoms.

A graphene flake of square shape is introduced into the grain boundary. It has a side length of 34 nm and is aligned with the lattice of the lower Ni block.

Structures containing graphene in the grain boundary will be denoted as g (graphene) systems, while elemental Ni systems will be denoted as hm (homointerface) systems.

We use the Mishin potential [13] to model the Ni-Ni interactions and the AIREBO potential [23] for the C-C interactions. The interaction between Ni and C is modeled by a Lennard-Jones potential according to Ref. [7].

The indenter is modeled non-atomistically as a spherical tip of radius 5 nm. It interacts with the substrate atoms via a repulsive potential according to the recipe of [8]. During the simulation, the indenter moves with a velocity of 20 m/s into the workpiece to a depth of 5 nm.

For each system, we perform 5 individual indentation simulations which differ from each other by the exact positioning of the indenter; it was moved in lateral direction randomly to another position by around ± 2 Å. Data shown are averages over these 5 simulations, unless specified otherwise.

In the Appendix 5, we also study how the orientation of the graphene flake with respect to the indentation direction influences the indentation process. For this purpose, graphene flakes oriented parallel to the indentation direction are introduced in the substrate.

The simulations are performed with the open-source code LAMMPS [18] using a constant time step of 1 fs.

3 Results

3.1 Influence of the depth of graphene

We display in Fig. 2 the forces exerted on a Ni-graphene composite during indentation to a depth of 5 nm. Three different depths of the graphene flake are compared with each other: (i) 3 nm – here the indenter touches the flake during indentation; (ii) 5 nm – here the flake is only touched at the deepest point of indentation; (iii) 8 nm – the indenter never touches the flake. Note that the figure shows averages over 5 simulations, since it is known that individual indentation events – differing by the exact indentation point – may vary from each other due to the statistical nature of dislocation generation and movement [26].

Results are shown in Fig. 2b for two different grain boundaries: for a strong grain boundary – the 60° twist grain boundary – in Fig. 2a and for a weak grain boundary – the 30° twist grain boundary. We first discuss the data for the strong grain boundary, Fig. 2a. Apart from statistical fluctuations, the data show astonishingly little difference. In particular, when the indenter touches the interface for the $h = 3$ nm flake, the curves remain unaffected. Only at depths > 3 nm, after the indenter touched the interface and starts bending down the graphene flake, the force required for indentation for the $h = 3$ nm flake is largest. The force-depth curves for the graphene flakes positioned deeper inside the Ni matrix, 5 and 8 nm, show no differences.

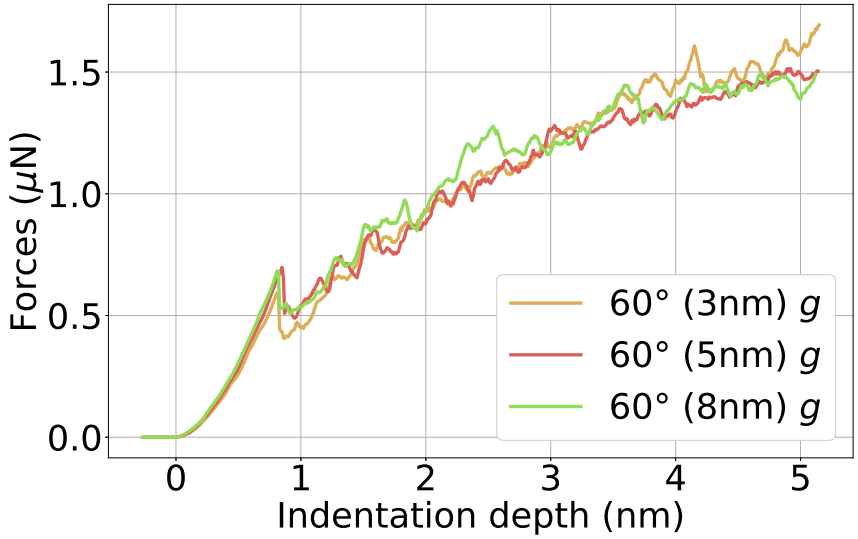

(a)

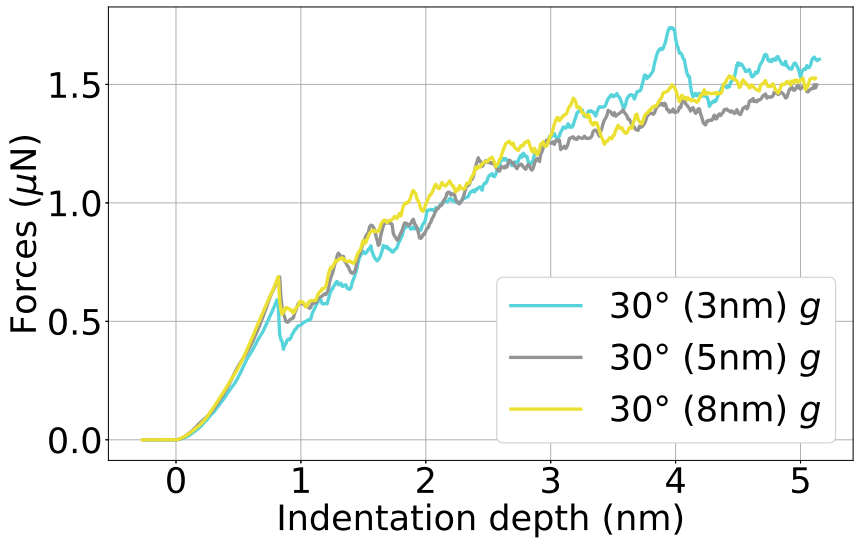

(b)

Figure 2 Force-depth curves for indentation in a Ni bi-crystal containing a (a) 60° and (b) 30° twist grain boundary coated with graphene. Data are shown for three different depths h (3, 5, and 8 nm) of the grain boundary.

The results are similar for the the weak 60° twist grain boundary, Fig. 2b. Again the indentation forces required for graphene flakes positioned at various depths are quite similar to each other. Only for the shallowest flake, situated a 3 nm, a strong increase in force is seen at the indentation depth of 4 nm, after the indenter touched the flake. A detailed analysis of the plastic processes inside the sample [26] shows that the peak is caused by stress increase immediately before dislocations are generated in the lower Ni block; the generation of plasticity then partially relieves the stress.

For both bi-crystal systems, a systematic influence of the graphene depth shows up at the position of the first load drop, at around 0.8 nm. This load drop is caused by the emission of dislocations due to the high stresses caused by the indenter; the creation of these defects partially releases the stress and leads to the load drop. However, the created dislocations already touch the flake in the case the shallowest flake situated at 3 nm depth; this leads to the smaller indentation force in this case.

We conclude that the exact positioning of the graphene flake beneath the indenter has only a small influence on the force of the indenter. Only when the indenter touches the graphene, and at the initial load drop, when dislocations are generated, the exact position of the flake is relevant.

3.2 Influence of graphene size and orientation

The graphene flake used up to now had a square shape of side length 34 nm, and was aligned with the (111) surface of the lower Ni block. In the following we will focus on the Ni bi-crystal containing a 60° twist grain boundary at a depth of 3 nm, and will denote this setting as the "standard case". In Figs. 3 and 4, we vary the size and exact positioning of the graphene flake and study its consequences on the indentation force. The "standard case" simulations are included in these plots as a reference; individual results are shown in order to allow to asses their variance.

Fig. 3a gives an example of how the indentation force varies, if the lateral position of the graphene flake is slightly changed by ± 2 Å. Note that due to the lattice mismatch between graphene and the Ni(111) surface of 2.9 %, the graphene lattice is incongruent with the Ni(111) surface and so there is no "optimum" lateral positioning (on the atomic scale) which minimizes the interaction energy. However, this figure shows us that a different lateral graphene position does not change the response of the composite to indentation in any statistically relevant manner.

Fig. 3b studies a second issue, namely the orientation of the graphene flake. In the standard case, we assumed that the flake is oriented with respect to the lower Ni block. We now introduce a misorientation of 30°; this corresponds to a maximum misorientation, since for a rotation by 60°, the flake would be aligned with the upper Ni block. Again, the figure shows no statistically relevant effect on the indentation force. This may appear surprising since the graphene flake is now misaligned both with respect to the upper and the lower Ni block. However, since the interface is incoherent anyway, even a rotation of the graphene flake does not disturb the performance of the interface under indentation.

Finally, we investigate the influence of the size of the flake on the force-depth curves. On the one extreme, we expanded the flake laterally infinitely, thus mimicking a macroscopically large graphene sheet. This was achieved by extending the graphene flake to the edges of the simulation volume and using laterally periodic boundary conditions. As Fig. 4a shows, the results are statistically indistinguishable from a finite flake of side length 34 nm. Only when the indenter touches the flake, the "infinite" sheet shows a higher resistance, as demonstrated by its increased force. This is because bending of the interface – which has to occur after the indenter touched the interface, since the graphene is too strong to tear – is more difficult for the larger flake.

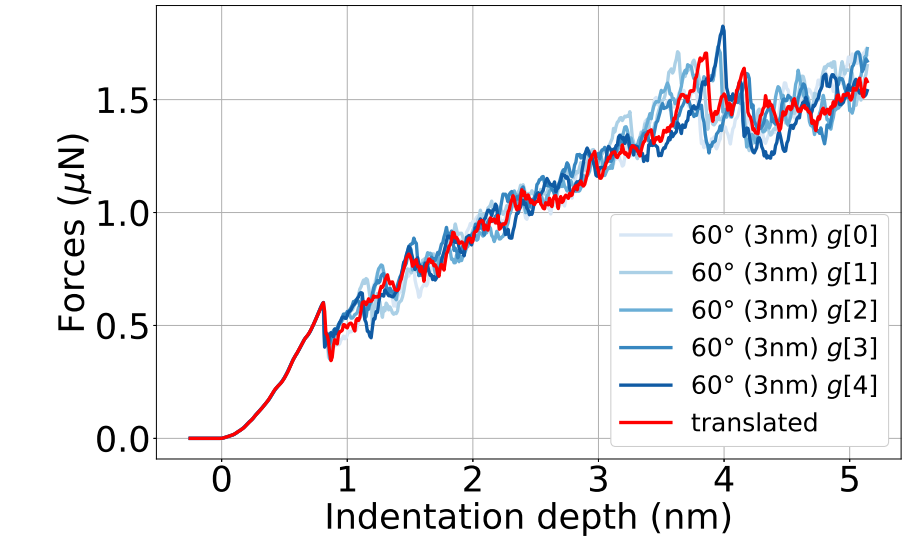

(a)

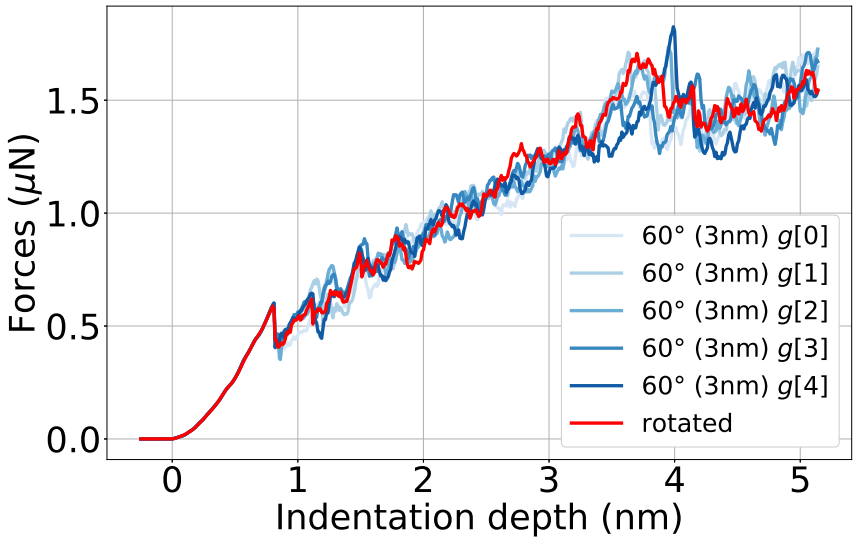

(b)

Figure 3 Force-depth curves for indentation in a Ni bi-crystal containing a 60° twist grain boundary coated with graphene. Results are shown for a flake (a) with varied lateral position, (b) rotated by 30°, (c) with laterally infinite size, as mimicked by periodic boundaries, and (d) for a smaller flake of edge length 10 nm. Simulation data are compared to individual indentation results of the standard case.

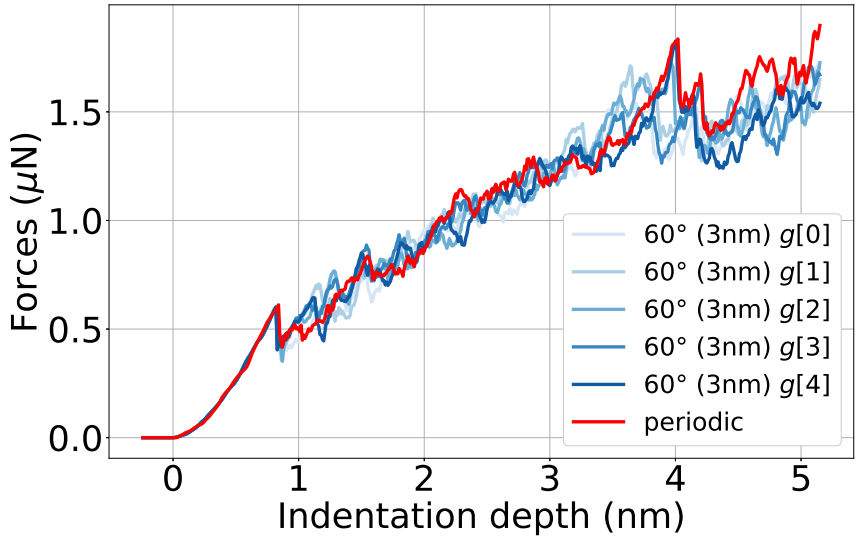

(a)

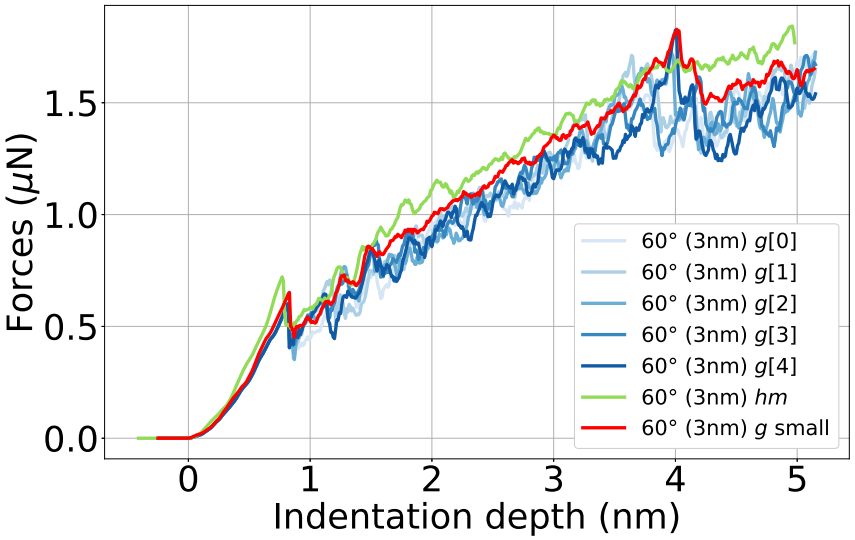

(b)

Figure 4 As in Fig. 3, but for a flake (a) with laterally infinite size, as mimicked by periodic boundaries, and (b) for a smaller flake of edge length 10 nm. Simulation data are compared either to individual indentation results of the standard case (a), or with averages of the results of standard cases (b).

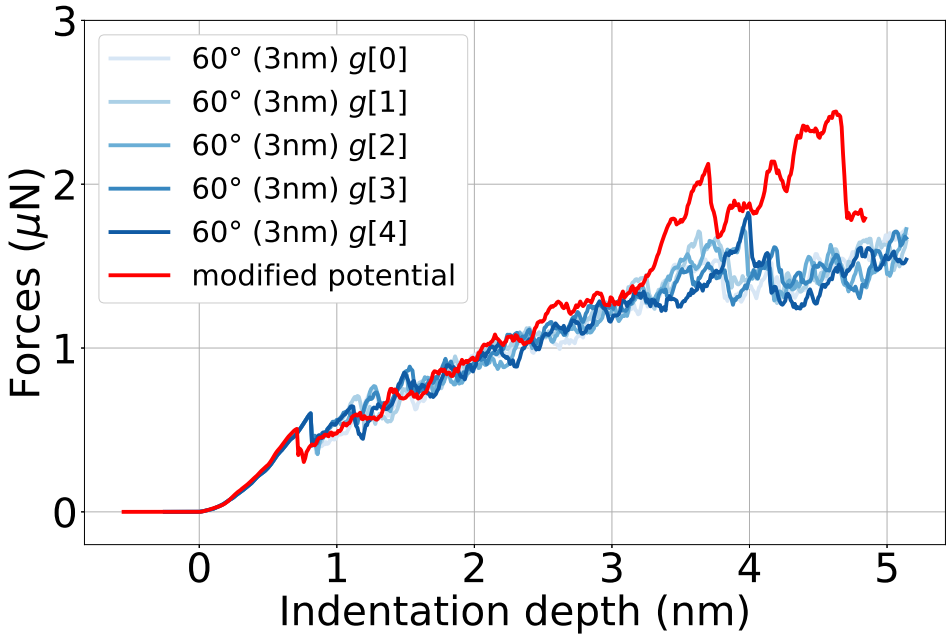

Figure 5 Force-depth curve for indentation into a 60° grain boundary at 3 nm depth coated by graphene. The results of a changed Ni-graphene potential are compared to individual indentation results for the standard case.

On the other hand, we decreased the size of the flake to only 10 nm × 10 nm. Here, the simulation (Fig. 4b) shows a hardening as compared to the standard flake size of 34 nm, but the hardening does not quite reach the values of the pure Ni sample. The general decrease of the force – compared to the pure Ni case – before the indenter touches the graphene is caused by the absorption of dislocations in the interface [25, 26]. A smaller flake can absorb only fewer dislocations such that with decreasing size of the graphene flake, the results continuously converge to those of the case of elemental Ni. After the indenter touched the interface, at around 4 nm indentation depth, we see a force maximum followed by a sharp decrease, which is reminiscent of the behavior of the 30° twist boundary, see Fig. 2b. This occurs because dislocations start nucleating in the lower Ni block and release the stress that has built up.

We conclude that the exact positioning of the graphene flake and its orientation do not alter the performance of the composite during indentation, since the quality of the incoherent interface cannot deteriorate further. On the other hand, its size matters to some extent. Smaller flakes show increased strength, since less dislocations are absorbed in the interface. Larger flakes, however, only show changes when the indenter touches the interface; they then appear harder since graphene bending is rendered more difficult. This demonstrates that our size of 34 nm was chosen well for studying the effects of large flakes under indentation.

3.3 Influence of the Ni-graphene interaction potential

The interaction between graphene and the surrounding metal is usually modeled by a simple Lennard-Jones (LJ) potential [7, 2, 10, 16, 29],

$$V(r) = 4\varepsilon \left[\left(\frac{\sigma}{r}\right)^{12} - \left(\frac{\sigma}{r}\right)^{6} \right]. \tag{1}$$

This simple interaction presumes that all covalent bonds within graphene are saturated such that the C atoms will only have van-der-Waals interactions with the surrounding metal. We follow here the argumentation of Huang *et al.* [7] that the C-Ni interaction is at least one order of magnitude smaller than that of the Ni-Ni interaction. This paper recommends the LJ parameters $\varepsilon = 23.049$ meV and $\sigma = 2.852$ Å.

We now study the sensitivity of our results towards changes in the potential parameters for the Ni(111) surface. Indeed, several ab-initio calculations studied the complexities of the Ni-graphene interaction. Khomyakov *et al.* [9] find that the interaction involves the formation of chemical bonds that induce hybridization between graphene p_z states and metal d states. Tavazza *et al.* [24], using DFT calculations of the interaction of a C tip to a Ni surface, calculated a LJ potential [24] with $\varepsilon = 200$ meV and a length parameter of $\sigma = 1.514$ Å. This potential actually implements a strong covalent NiC bond; the atom distance ($2^{1/6}\sigma = 1.70$ Å) is close to that of a NiC dimer, 1.62 Å. We use this potential as an extreme case to illustrate the consequences of strong bonding, even though it will be unrealistic for a Ni-graphene sheet interaction.

The results for the changed Ni-C interaction are shown in Fig. 5. We see that before the tip touches the graphene, the force is not affected by the changed potential. However, upon direct contact, the indenter force strongly rises. This occurs, since the covalent strong interaction between Ni and graphene effectively increases the stiffness of the graphene sheet and requires a stronger force of the indenter to bend it. This result is in agreement with previous results [25] for the Ni(100) surface which showed that while an increase of the bond strength does not change the indentation behavior, a decrease of the length parameter lets the indentation force increase, since then the repulsive part of the Ni-C Lennard-Jones potential can transfer larger forces.

We conclude that even strong bonds between graphene and Ni – which might occur in a situation where graphene is highly defective, since graphene edge atoms might develop covalent bonds to the metal – change the hardness of the composite only when the indenter touches the graphene. Then the strong bonding adds to the out-of-plane stiffness of graphene and thus to the hardness of the composite.

4 Conclusions

We studied nanoindentation into a Ni bi-crystal containing a graphene sheet. We obtained the following findings.

1. The depth at which the graphene flake is positioned has surprisingly little effect on the indentation force. However, when the indenter touches the flake, the indentation increases due to a stress increase caused by the difficulty to nucleate dislocations in the lower Ni block. Also at the initial load drop, when dislocations are generated, the exact position of the flake is relevant.
2. Since the Ni-graphene interface is incoherent, small changes in the exact (atomic-scale) lateral positioning of the flake, and even rotations with respect of the orientation of the Ni(111) lattice have negligible effects on the indentation behavior.
3. When graphene flakes are smaller in size, the indentation force approaches that of the elemental Ni crystal; the effect of graphene diminishes. On the other hand, if a graphene sheet with periodic boundary conditions is used – so as to approximate a flake of macroscopic extension – the indentation force increases as soon as the indenter is touched, since bending of the graphene becomes more difficult.

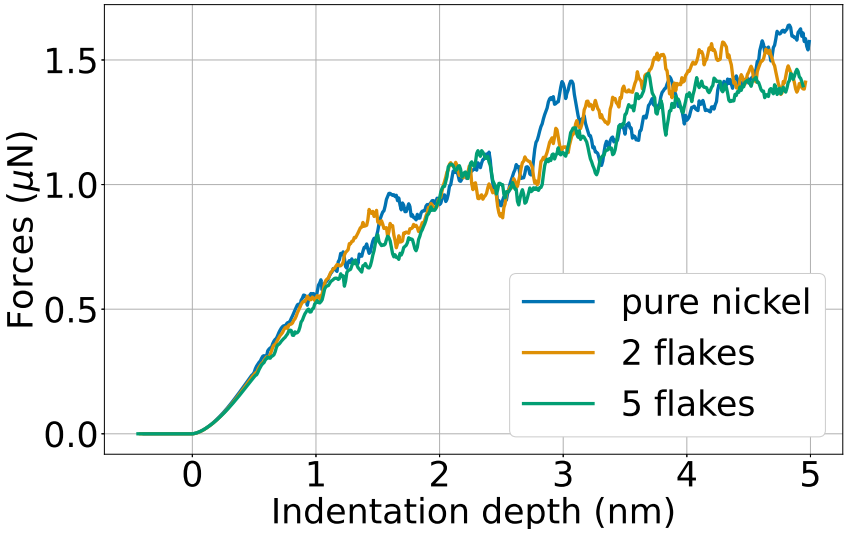

Figure 6 Force-depth curves for indentation in a Ni crystal containing vertical graphene flakes. Data are shown for three different systems: pure Ni, Ni containing 2 graphene flakes and Ni containing 5 graphene flakes.

4. In simulations, usually a pairwise interaction potential between the C atoms of the graphene flake and the Ni atoms is assumed, which models van-der-Waals-like interactions. When changing the potential to a stronger covalent-like bonding, indentation results are only affected when the indenter touches the graphene. The composite then appears harder, since bending of the graphene flake requires higher forces.

5 Vertical orientation of the graphene

In the present study as well as in previous computational work [2, 11, 31, 29, 6, 25, 26], the graphene flake is oriented parallel to the substrate surface and thus perpendicular to the indentation direction. However, it might be expected that the orientation of the graphene plane with respect to the indentation direction exerts a strong influence on the mechanical behavior. In order to study this influence, we investigate in this Appendix the extreme case, where the graphene flakes are oriented parallel to the indentation force and thus perpendicular to the surface. We simulate two scenarios: two graphene flakes placed at a distance of 20 nm positioned symmetrically such that the indenter does not touch them, and five graphene flakes at a distance of 5 nm positioned such that the indenter touches one of them at deepest penetration. The graphene flakes are embedded in single-crystalline Ni; they do not reach the surface, but end sufficiently far from the surface that the indenter touches them only at full penetration.

Fig. 6 displays the force-depth curves of these systems and compares them to the case of pure Ni. The effect of the flakes on the force evolution is indeed minor. In particular, the 2-flakes system shows a behavior that is – apart from the noise that is generated by the statistical fluctuations of dislocation generation – quite close to that of the pure-Ni system. The 5-flake system appears to be somewhat weaker than the others. This weakening is already seen quite early, at indentation depths below 1 nm; here the presence of graphene

allows for an easier nucleation of dislocations. Since dislocation generation releases the stress in the sample, the force acting on the indenter decreases. At larger indentation depths, when dislocations may glide easily along the flakes away from the indenter, the force in the 5-flake case is slightly smaller (in average) than in the other cases.

A detailed inspection of the simulation results shows that the dislocation network generated by the indentation is constrained laterally by the graphene flakes; however, the depths reached by the dislocations are similar in all cases, since dislocation propagation into the crystal interior is not blocked by graphene in this geometry. Dislocations are not repelled by the flakes but may extend to them resulting in lateral displacements of graphene atoms similar to what was described earlier in the literature [25]. In addition, the Ni dislocations can easily glide along the graphene flakes downward in the course of the indentation. Thus, while the flakes hinder the lateral expansion of the dislocations from their point of generation near the indenter, the dislocations may move freely downward and thus release the stress build-up by the indenter. This feature explains the negligible influence of the graphene flakes on the force-depth curve, Fig. 6, in this orientation.

We conclude that the vertical arrangement of graphene flakes only little influences the indentation behavior of Ni, and leads to only a slight weakening of the sample. This is caused by the fact that Ni dislocations – once they got attached to the flakes – can glide easily along them. Thus the effect of graphene on the indentation behavior in this geometry is even smaller than with the flakes oriented perpendicular to the indentation direction, where the flakes are able to block the dislocation propagation towards the material interior.

References

1 R. W. Armstrong, W. L. Elban, and S. M. Walley. Elastic, plastic, cracking aspects of the hardness of materials. *Int. J. Mod. Phys. B*, 27:1330004, 2013.

2 Shu-Wei Chang, Arun K. Nair, and Markus J. Buehler. Nanoindentation study of size effects in nickel-graphene nanocomposites. *Philosophical Magazine Letters*, 93(4):196–203, 2013. doi:10.1080/09500839.2012.759293.

3 Qing Feng, Xiaoyan Song, Hongxian Xie, Haibin Wang, Xuemei Liu, and Fuxing Yin. Deformation and plastic coordination in wc-co composite–molecular dynamics simulation of nanoindentation. *Materials & Design*, 120:193–203, 2017. doi:10.1016/j.matdes.2017.02.010.

4 A. C. Fischer-Cripps. *Nanoindentation*. Springer, New York, 2 edition, 2004.

5 Qiang Guo, Katsuyoshi Kondoh, and Seung Min Han. Nanocarbon-reinforced metal-matrix composites for structural applications. *MRS Bulletin*, 44(1):40–45, 2019. doi:10.1557/mrs.2018.321.

6 Xin He, Qingshun Bai, and Rongqi Shen. Atomistic perspective of how graphene protects metal substrate from surface damage in rough contacts. *Carbon*, 130:672–679, 2018. iron. doi:10.1016/j.carbon.2018.01.023.

7 Shi-Ping Huang, D. S. Mainardi, and P. B. Balbuena. Structure and dynamics of graphite-supported bimetallic nanoclusters. *Surface Science*, 545:163–179, 2003. doi:10.1016/j.susc.2003.08.050.

8 C. L. Kelchner, S. J. Plimpton, and J. C. Hamilton. Dislocation nucleation and defect structure during surface indentation. *Phys. Rev. B*, 58:11085–11088, 1998.

9 P. A. Khomyakov, G. Giovannetti, P. C. Rusu, G. Brocks, J. van den Brink, and P. J. Kelly. First-principles study of the interaction and charge transfer between graphene and metals. *Phys. Rev. B*, 79:195425, May 2009. doi:10.1103/PhysRevB.79.195425.

10 Youbin Kim, Jinsup Lee, Min Sun Yeom, Jae Won Shin, Hyungjun Kim, Yi Cui, Jeffrey W. Kysar, James Hone, Yousung Jung, Seokwoo Jeon, and Seung Min Han. Strengthening effect of single-atomic-layer graphene in metal-graphene nanolayered composites. *Nat. Commun.*, 4:2114, 2013. doi:10.1038/ncomms3114.

11 Da Kuang, Liye Xu, Lei Liu, Wenbin Hu, and Yating Wu. Graphene-nickel composites. *Applied Surface Science*, 273:484–490, 2013. doi:10.1016/j.apsusc.2013.02.066.

12 XiaoYi Liu, FengChao Wang, WenQiang Wang, and HengAn Wu. Interfacial strengthening and self-healing effect in graphene-copper nanolayered composites under shear deformation. *Carbon*, 107:680–688, 2016. doi:10.1016/j.carbon.2016.06.071.

13 Y. Mishin, D. Farkas, M. J. Mehl, and D. A. Papaconstantopoulos. Interatomic potentials for monoatomic metals from experimental data and ab initio calculations. *Phys. Rev. B*, 59:3393, 1999.

14 A Misra, J P Hirth, and R G Hoagland. Length-scale-dependent deformation mechanisms in incoherent metallic multilayered composites. *Acta Mater.*, 53(18):4817–4824, 2005. doi:10.1016/j.actamat.2005.06.025.

15 S. E. Muller and A. K. Nair. Dislocation nucleation in nickel-graphene nanocomposites under mode i loading. *JOM*, 68:1–6, 2016. doi:10.1007/s11837-016-1941-y.

16 Scott E. Muller, Raghuram R. Santhapuram, and Arun K. Nair. Failure mechanisms in pre-cracked ni-graphene nanocomposites. *Computational Materials Science*, 152:341–350, 2018. doi:10.1016/j.commatsci.2018.06.013.

17 David L. Olmsted, Stephen M. Foiles, and Elizabeth A. Holm. Survey of computed grain boundary properties in face-centered cubic metals: I. grain boundary energy. *Acta Materialia*, 57(13):3694–3703, 2009. doi:10.1016/j.actamat.2009.04.007.

18 St. Plimpton. Fast parallel algorithms for short-range molecular dynamics. *J. Comput. Phys.*, 117:1–19, 1995. *http://lammps.sandia.gov/*.

19 T. Ramanathan, A. A. Abdala, S. Stankovich, D. A. Dikin, M. Herrera-Alonso, R. D. Piner, D. H. Adamson, H. C. Schniepp, X. Chen, R. S. Ruoff, S. T. Nguyen, I. A. Aksay, R. K. Prud'Homme, and L. C. Brinson. Functionalized graphene sheets for polymer nanocomposites. *Nature nanotechnology*, 3(6):327, May 2008. doi:10.1038/nnano.2008.96.

20 Carlos J. Ruestes, Iyad Alabd Alhafez, and Herbert M. Urbassek. Atomistic studies of nanoindentation – a review of recent advances. *Crystals*, 7:293, 2017. doi:10.3390/cryst7100293.

21 Carlos J Ruestes, Eduardo M Bringa, Yu Gao, and Herbert M Urbassek. Molecular dynamics modeling of nanoindentation. In Atul Tiwari and Sridhar Natarajan, editors, *Applied Nanoindentation in Advanced Materials*, chapter 14, pages 313–345. Wiley, Chichester, UK, 2017. doi:10.1002/9781119084501.ch14.

22 Fei Shuang and Katerina E. Aifantis. Relating the strength of graphene/metal composites to the graphene orientation and position. *Scripta Materialia*, 181:70–75, 2020. doi:10.1016/j.scriptamat.2020.02.014.

23 S. J. Stuart, A. B. Tutein, and J. A. Harrison. A reactive potential for hydrocarbons with intermolecular interactions. *J. Chem. Phys.*, 112:6472–6486, 2000.

24 Francesca Tavazza, Thomas P Senftle, Chenyu Zou, Chandler A Becker, and Adri C. T. van Duin. Molecular dynamics investigation of the effects of tip-substrate interactions during nanoindentation. *J. Phys. Chem. C*, 119:13580–13589, 2015.

25 Vardan Hoviki Vardanyan and Herbert M. Urbassek. Dislocation interactions during nanoindentation of nickel-graphene nanocomposites. *Computational Materials Science*, 170:109158, 2019. doi:10.1016/j.commatsci.2019.109158.

26 Vardan Hoviki Vardanyan and Herbert M. Urbassek. Strength of graphene-coated ni bicrystals: A molecular dynamics nano-indentation study. *Materials*, 13(7):1683, 2020. doi:10.3390/ma13071683.

27 Shayuan Weng, Huiming Ning, Tao Fu, Ning Hu, Yinbo Zhao, Cheng Huang, and Xianghe Peng. Molecular dynamics study of strengthening mechanism of nanolaminated graphene/cu composites under compression. *Scientific Reports*, 8(1):3089, 2018.

28 Ding-Bang Xiong, Mu Cao, Qiang Guo, Zhanqiu Tan, Genlian Fan, Zhiqiang Li, and Di Zhang. Graphene-and-copper artificial nacre fabricated by a preform impregnation process: bioinspired strategy for strengthening-toughening of metal matrix composite. *ACS Nano*, 9(7):6934–6943, 2015. doi:10.1021/acsnano.5b01067.

29 Yuping Yan, Shangru Zhou, and Sheng Liu. Atomistic simulation on nanomechanical response of indented graphene/nickel system. *Computational Materials Science*, 130:16–20, 2017. doi:10.1016/j.commatsci.2016.12.028.

30 Zhenyu Yang, Dandan Wang, Zixing Lu, and Wenjun Hu. Atomistic simulation on the plastic deformation and fracture of bio-inspired graphene/ni nanocomposites. *Applied Physics Letters*, 109(19):191909, 2016. doi:10.1063/1.4967793.

31 Fatemeh Yazdandoost, Ayoub Yari Boroujeni, and Reza Mirzaeifar. Nanocrystalline nickel-graphene nanoplatelets composite: Superior mechanical properties and mechanics of properties enhancement at the atomistic level. *Phys. Rev. Materials*, 1:076001, December 2017. doi:10.1103/PhysRevMaterials.1.076001.

32 Peng Zhang, Lulu Ma, Feifei Fan, Zhi Zeng, Cheng Peng, Phillip E. Loya, Zheng Liu, Yongji Gong, Jiangnan Zhang, Xingxiang Zhang, Pulickel M. Ajayan, Ting Zhu, and Jun Lou. Fracture toughness of graphene. *Nature Communications*, 5:3782 EP–, April 2014.